

Nonlinear dynamics of aqueous dissolution of silicate materials

Yifeng Wang

Sandia National Laboratories, P. O. Box 5800, Albuquerque, New Mexico 87185-0779, USA
ywang@sandia.gov

Abstract:

Aqueous dissolution of silicate materials exhibits complex temporal evolution and rich pattern formations. Mechanistic understanding of this process is critical for the development of a predictive model for a long-term performance assessment of silicate glass as a waste form for high-level radioactive waste disposal. Here we provide a summary of a recently developed nonlinear dynamic model for silicate material degradation in an aqueous environment. This model is based on a simple self-organizational mechanism: dissolution of silica framework of a material is catalyzed by cations release from material degradation, which in turn further accelerates the release of cations. This model provides a systematical prediction of the key features observed in silicate glass dissolution, including the occurrence of a sharp corrosion front, oscillatory dissolution, multiple stages of the alteration process, wavy dissolution fronts, growth rings, incoherent bandings of alteration products, and corrosion pitting. This work provides a new perspective for understanding silicate material degradation and evaluating the long-term performance of these materials as a waste form for radioactive waste disposal.

Introduction

Silicate materials can be found in numerous industrial and technological applications including molecular sieves for chemical separation, catalysts for chemical conversion [1], optical fibers for communication [2], biomedical devices [3], construction materials [4], and waste forms for nuclear waste disposal [5-6]. In many of such applications, the chemical reactivity of a material with water directly determines the lifetime of the material in service. Thus, understanding chemical alteration of these materials in aqueous environments is particularly important for material development and their potential applications, especially for radioactive waste disposal, which requires the performance of a material to be evaluated for an extended period up to hundreds of thousand years [5-6]. Over such time scales, any model prediction of material performance must be footed on a mechanistic understanding of the underlying processes.

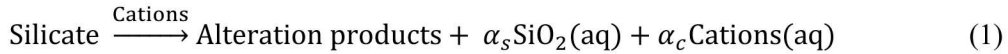
The underlying mechanism for the dissolution remains controversial. The debate has centered on the possible formation of a leached surface layer and its role in material dissolution. A silica-rich surface layer has been detected on both manufactured and natural silicate materials [7-9]. Alkali and alkaline cations in this layer are partially leached out and replaced by hydrogen ions through a coupled diffusion-ion exchange process. The leached layer may be subjected to in-situ silicate network reorganization, leading to the formation of a dense silica gel layer that may passivate a dissolving solid surface [10]. However, this view has been challenged by the observations of extremely sharp interfaces between altered rims and pristine material domains [11-14] and oscillatory zonings in the altered rims [15-17], suggesting that material

corrosion may undergo a direct dissolution-precipitation process. Oscillatory zonings on archeologic glass samples have been attributed to seasonal fluctuations in temperature or hydrologic conditions [18]. But this explanation is apparently not applicable to laboratory experiments, which are usually conducted under static conditions with no externally imposed periodic changes in experimental conditions. Thus, the observed oscillatory dissolution behaviors must be self-organizational, i.e., originated from the internal dynamics of solid-water interactions.

Results

Self-organizational mechanism

Self-organization requires a positive feedback among physical and chemical processes involved in a system. Wang and his colleagues have proposed the following positive feedback [19]: As a silicate material corrodes, cations (notably Na^+) in the material are released into the solution, resulting in a local high cation concentration and pH at the reaction front. Under alkaline conditions, silicate dissolution is catalyzed by both hydroxyl groups and cations. The resultant high pH and cation concentration enhance silicate material dissolution, which in turn accelerates cation release. The overall dissolution-precipitation reaction process can stoichiometrically be represented by reaction (1) [20]:



where α_s and α_c are the stoichiometric coefficients of dissolved SiO_2 and cations, respectively, in the overall silicate alteration reaction. Since most of SiO_2 released from the dissolution is re-incorporated into the alteration products, α_s is relatively small compared to α_c . The cations in reaction (1) refer to alkali cations (mainly Na^+) and part of alkaline-earth cations that remain as dissolved cationic species in solution after their release from material degradation.

Mathematical model

Let's consider a modeling system as illustrated in Fig. 1. The dissolved species released from the alteration communicate with the bulk solution via diffusion through the alteration products. Assume that the position of the dissolution front at time t can be described by $X = F(Y, t)$. The evolution of the glass dissolution front can be described by the following dynamic equations [20]:

For $F(Y, t) < X < L$:

$$\frac{\partial C_s}{\partial t} = D_s \nabla^2 C_s \quad (2)$$

$$\frac{\partial C_c}{\partial t} = D_c \nabla^2 C_c \quad (3)$$

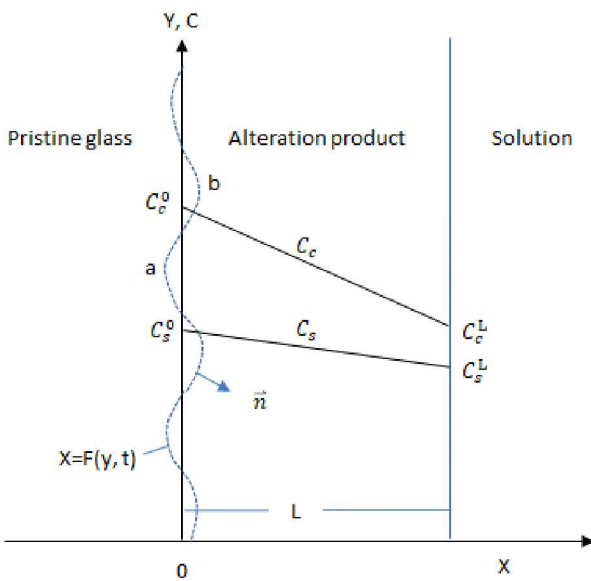


Fig. 1. Schematic representation of the system for silicate material degradation [19]. Vertical axis represents both Y coordinate and the concentrations of dissolved species. The dashed line indicates a small perturbation introduced to an initially planar dissolution surface.

where X and Y are the spatial coordinates (Fig. 1); $F(Y, t)$ describes the location of the dissolution front; t is the time; C_s and C_c are the concentrations of dissolved SiO_2 and cations, respectively; D_s and D_c are the effective diffusion coefficients of the two species, respectively; and L is the thickness of the alteration zone.

At $X = F(Y, t)$:

$$\alpha_s R = -D_s \vec{\nabla} C_s \cdot \vec{n} \quad (4)$$

$$\alpha_c R = -D_c \vec{\nabla} C_c \cdot \vec{n} \quad (5)$$

$$R = k \left[1 + \beta \left(\frac{C_c}{C_{IEP}} \right)^m \right] (C_s^e - C_s) \quad (6)$$

$$C_s^e = C_s^e(\infty)(1 + \Gamma K) \quad (7)$$

$$K = -\frac{\partial^2 F}{\partial Y^2} / \left[1 + \left(\frac{\partial F}{\partial Y} \right)^2 \right]^{3/2} \quad (8)$$

$$\vec{n} = \left(1, -\frac{\partial F}{\partial Y} \right)^T / \left[1 + \left(\frac{\partial F}{\partial Y} \right)^2 \right]^{1/2} \quad (9)$$

where \vec{n} is the normal vector of the dissolution front pointing toward the alteration zone; R is the dissolution rate; k is the reaction rate constant; β and m are constants characterizing the catalytic effect of cations on the dissolution rate of silica framework; C_{IEP} is the concentration of cations at the isoelectric point; C_s^e is the solubility of silica framework on a surface of curvature K ; $C_s^e(\infty)$ is the solubility of silica framework on a planar surface; Γ is the surface tension of the interface between the pristine glass and the solution; and superscript “ T ” in Eq. (9) represents the transposition of a vector. Equations (7) and (8) capture the effect of surface tension on the solubility of silica framework.

At $X = L$:

$$C_s = C_s^L \quad (10)$$

$$C_c = C_c^L \quad (11)$$

The kinematics of the dissolution front can be described by:

$$\rho \frac{\partial F}{\partial t} = \bar{R} - R \left[1 + \left(\frac{\partial F}{\partial Y} \right)^2 \right]^{1/2} \quad (12)$$

$$\bar{R} = k \left[1 + \beta \left(\frac{\bar{C}_c}{C_{IEP}} \right)^m \right] [C_s^e(\infty) - \bar{C}_s] \quad (13)$$

where ρ is the molar density of the silicate material; \bar{R} is the reaction rate evaluated at the planar front; and \bar{C}_c and \bar{C}_s are the concentrations of dissolved SiO_2 and cations at the planar front, respectively.

Oscillatory dissolution

Equations (2) through (13) have been solved numerically for a planar dissolution front [19,20]. The model simulations show that, under certain model parameter ranges, the concentrations of both cation and dissolved silica at the dissolution front can oscillate out of phase with time (Fig. 2), even if the concentrations in the bulk solution outside the alteration products remain constant, and so do the glass dissolution rate and the rate of alteration product precipitation, resulting in repetitive chemical or structural bandings in alteration products [15-18]. Through a model analysis, the time scale for each oscillation is estimated to range from hours to a year, consistent with observations [15,16,18]. Similarly, the scale of each band is estimated to be sub-micrometers to micrometers, again consistent with observations [12,16]. The thickness of each band is expected to be roughly the time scale for each oscillation multiplied by the diffusional flux of mass across the alteration product layer, with the former proportional to the thickness of the alteration layer (L) while the latter inversely proportional to L [19]. Consequently, the thickness of each band should remain relatively constant as L evolves during material degradation. Apparently, the bands formed as such do not follow a spacing law for a typical Liesegang banding [21].

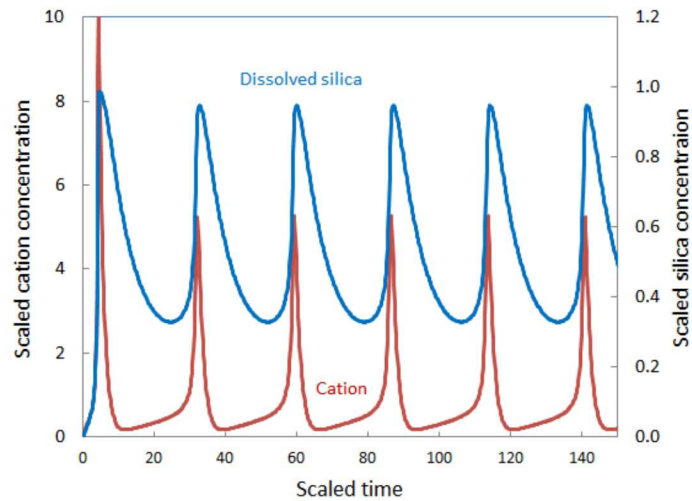
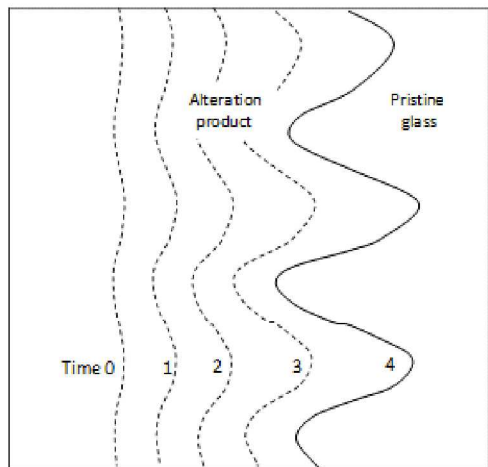
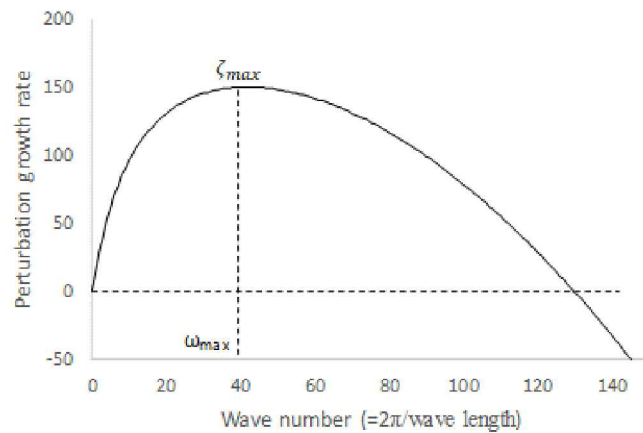


Fig. 2. Predicted concentration oscillations at the glass dissolution interface [17].



A



B

Fig. 3. Morphological instability of dissolution front induced by the proposed self-organizational mechanism. A. Schematic illustration of the evolution of an unstable dissolution front. B. Growth rate of perturbation as a function of the wave number of perturbation.

Morphological instability of dissolution front

Let's assume that the dissolution of a silicate material starts on a planar reaction front (Fig. 1). In an actual system, the front is inevitably subjected to environmental perturbations, resulting in small fluctuations in reaction rate on the dissolution front. Based on the self-organizational mechanism proposed above, in a faster dissolution location (labeled "a" in Fig. 1), more cations would be released and accumulated, which in turn further accelerates the dissolution at this location. The opposite happens at location "b", where the cations can be relatively easier to diffuse away due to a shorter diffusion distance through the alteration zone (Fig. 1). Consequently, a small perturbation to an initially planar front can be amplified, leading to the formation of a wavy front (Fig. 3A).

A linear stability analysis of equations (2) through (13) have been performed [20]. In this analysis, an infinitesimal perturbation of a given wave number is first introduced to an initially planar reaction front, and the growth rate of the perturbation is then determined as a function of wave number. A typical growth rate of perturbation as a function of wave number is shown in Fig. 3B. As shown in the figure, over a certain range of wave number, the growth rate of perturbation becomes positive, implying that the perturbations with these wave numbers can potentially be amplified, leading to the formation of a wavy dissolution front. The actual wave length of the front is determined by the wave number with a maximum growth rate (ω_{max}). The wave length is estimated to range from a few to hundreds of micrometers [20], consistent with observations [11-13,16].

As shown in Fig. 4, the interaction of oscillatory dissolution with morphological instability of the dissolution could lead to complex pattern formations in alteration products [20]. For example, if the growth rate of morphological perturbations is comparable with the rate of dissolution front advancement and the concentration oscillations excursion into a morphologically unstable field with narrowly ranged wavelengths, resulting in a set of coherent wavy bands (Figs. 4A and 4B). On a view plane parallel to the front, these wavy bandings can be expressed as concentric growth rings [16] (Fig. 4C). Also, if the growth rate of morphological perturbations is comparable with the rate of dissolution front advancement and the concentration oscillations cross over a morphologically unstable field with a wide range of wavelengths, leading to a set of incoherent alteration bands (Fig. 4D).

Zeolite formation and long-term glass dissolution rate

The proposed self-accelerating mechanism also provides a new perspective about zeolite formation in silicate glass dissolution and its relation to the long-term durability of the materials [20]. As the dissolution

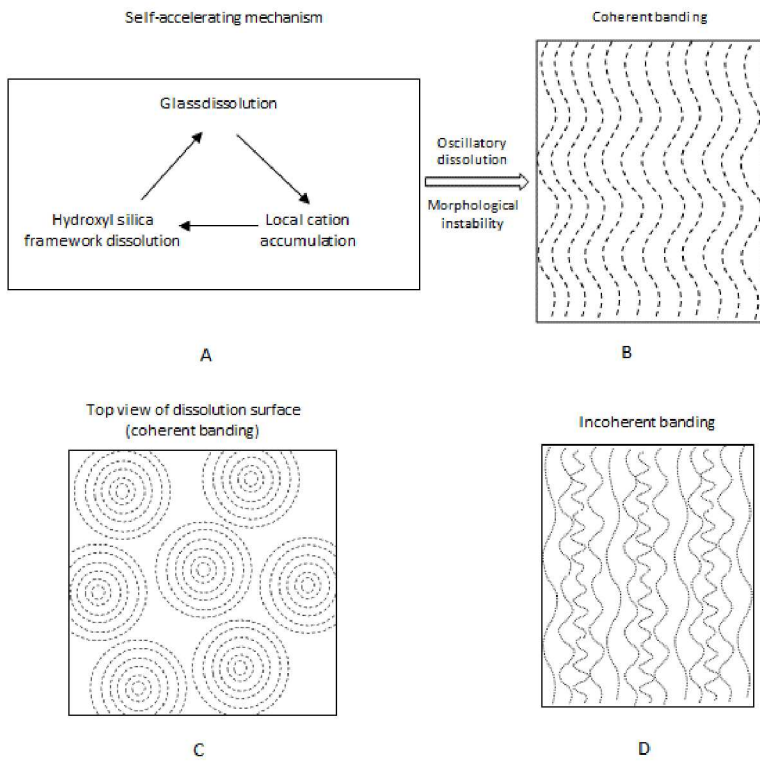


Fig. 4. Schematic illustration of the interaction of oscillatory dissolution with dissolution front instability leading to complex pattern formation.

proceeds, the dissolution rate increases as more cations accumulate in the boundary layer. Eventually, the dissolution rate overtakes the mass exchange rate, leading to a “runaway” situation with a sharp increase in the cation concentration at the interface and therefore the dissolution rate. The sharp increase in both cation concentration and pH inevitably causes zeolite precipitation. Therefore, contradicting the existing point of view that the zeolite precipitation causes alteration resumption [6], The self-accelerating concept suggests that zeolite formation is a consequence of the alteration resumption process. The precipitation of zeolite would eventually limit further increase in the reaction rate by removing cations from the dissolution front. Thus, the resumption rate may likely represent a long-term rate for silicate glass dissolution. Whether or how soon the alteration resumption occurs depends on glass composition. The durability of a glass can thus be engineered by choosing an appropriate glass recipe [20].

Conclusions

It has been shown that the observed complexity of silicate material degradation can emerge from a simple self-organizational mechanism. This mechanism enables us to systematically predict the key features observed in silicate glass dissolution, including the occurrence of a sharp corrosion front, oscillatory dissolution, multiple stages of the alteration process, wavy dissolution fronts, growth rings, incoherent bandings of alteration products, and corrosion pitting. This work provides a new perspective for understanding silicate material degradation and evaluating the long-term performance of these materials as a waste form for radioactive waste disposal.

Acknowledgements: Sandia National Laboratories is a multi-mission laboratory managed and operated by National Technology and Engineering Solutions of Sandia, LLC., a wholly owned subsidiary of Honeywell International, Inc., for the U.S. Department of Energy’s National Nuclear Security Administration under contract DE-NA-0003525. The work was supported by DOE Spent Fuel Waste Science & Technology (SFWST) Program.

- [1] Kulprathipanja, S. (ed.) *Zeolites in Industrial Separation and Catalysis* (Wiley-VCH, Weinheim, 2010).
- [2] Murata, H. *Handbook of Optical Fibers and Cables* (Marcel Dekker, New York, 1996).
- [3] Hin, T. S. *Engineering Materials for Biomedical Applications* (World Scientific Publishing Co, New Jersey, 2004).
- [4] Domone, P., Illston, J. *Construction Materials* (Spon Press, New York, 2010).
- [5] Cailleteau, C. et al. Insight into silicate-glass corrosion mechanisms. *Nature Materials* 7, 978-983 (2008).
- [6] Gin, S. Open scientific questions about nuclear glass corrosion. *Procedia Materials Sci.* 7, 163-171 (2014).
- [7] Dran, J.-C., Petit, J.-C., Brousse, C. Mechanism of aqueous dissolution of silicate glasses yield by fission tracks. *Nature* 319, 485-487 (1986).
- [8] Doremus, R. H. Interdiffusion of hydrogen and alkali ions in a glass surface. *J. Non-Crystalline Solids* 19, 137-144 (1975).
- [9] Petit, J.-C. et al. Paccagnella, A. Hydrated-layer formation during dissolution of complex silicate glasses and minerals. *Geochim. Cosmochim. Acta* 54, 1941-1955 (1990).
- [10] Gin, S. et al. Dynamics of self-reorganization explains passivation of silicate glass. *Nature Communications* 9, 2169 (2018).
- [11] Putnis, A. Sharpened interface. *Nature Materials* 14, 261-261 (2015).
- [12] Hellmann, R. et al. Nanometre-scale evidence for interfacial dissolution-reprecipitation control of silicate glass corrosion. *Nature Materials* 14, 307-311 (2015).
- [13] Ruiz-Agudo, E., Putnis, C. V., Rodriguez-Navarro, C., Putnis, A. Mechanism of leached layer formation during chemical weathering of silicate minerals. *Geology* 40, 947-950 (2012).

- [14] Geisler, T. et al. The mechanism of borosilicate glass corrosion revisited. *Geochim. Cosmochim. Acta* 158, 112-129 (2015).
- [15] Geisler, T. et al. Aqueous corrosion of borosilicate glass under acidic conditions: A new corrosion mechanism. *J. Non-Crystalline Solids* 356, 1458-1465 (2010).
- [16] Dohmen, L. et al. Pattern formation in silicate glass corrosion zones. *Int. J. Appl. Glass Sci.* 4, 357-370 (2013).
- [17] Jeong, G. Y. & Sohn, Y. K. Mineralogy and microtextures of basaltic glass alteration in hyaloastite, Jeju Island, Korea. *J. Analytical Sci. Tech.* 2, 12-22 (2011).
- [18] Brill, R. H. & Hood, H. P. A new method for dating ancient glass. *Nature* 189, 12-14 (1961).
- [19] Wang, Y., Jove-Colon, C. F., Kuhlman, K. L. Nonlinear dynamics and instability of aqueous dissolution of silicate glasses and minerals. *Scientific Reports* 6, 30256 (2016).
- [20] Wang, Y., Jove-Colon, C. F., Lenting, C., Icenhower, J., Kuhlman, K. L. Morphological instability of aqueous dissolution of silicate glasses and minerals. *NPJ Materials Degradation* 2, 27 (2018); doi:10.1038/s41529-018-0047-0.
- [21] Dee, G. T. Pattern produced by precipitation at a moving reaction front. *Phys. Rev. Letters* 57, 275-278 (1986).